SCIENCE CHINA
Physics, Mechanics & Astronomy

• Article •
Special Issue: Physical Mechanics

June 2012 Vol.55 No.6: 1118–1124
doi: 10.1007/s11433-012-4750-5

Analysis of the shape of heavy droplets on flat and spherical surface

WANG XueWei &YU Yang*

Biomechanics and Biomaterials Laboratory, Department of Mechanics, School of Aerospace Engineering, Beijing Institute of Technology, Beijing 100081, China

Received February 13, 2012; accepted April 11, 2012; published online April 27, 2012

In this study, a theoretical model was established for predicting the equilibrium shape of the droplet on flat and spherical surfaces. The theoretical equilibrium shape of heavy droplets could be obtained once contact angle and volume of droplets were given. It showed that the predictions of the theoretical flat model were in good agreement with the shape obtained by Surface Evolver when the contact angle is below 120° and the droplet size is on the order of capillary length. This available range will decrease and increase when the heavy droplet is on convex and concave spherical surface, respectively, in contrast to that on flat surface. The available range will decrease more for higher curvature of convex spherical surfaces.

equilibrium shape, heavy droplet, ellipsoidal model, Surface Evolver simulation

PACS number(s): 68.03.Cd, 68.08.Bc, 68.15.+e, 68.03.Hj

Citation: Wang X W, Yu Y. Analysis of the shape of heavy droplets on flat and spherical surface. Sci China-Phys Mech Astron, 2012, 55: 1118–1124, doi: 10.1007/s11433-012-4750-5

1 Introduction

The shape of a droplet is critical to wetting and spreading behavior which has attracted considerable research because of its application in MEMS, medical equipment, electronic technology, chemistry, glass industry and biology [1–11]. The key parameters of droplets, including inner pressure, height and contact area on the surface, mainly depend on the equilibrium shape of the droplet. The inner pressure is an important factor to the wetting states (Wenzel state or Cassie-Baxter state) of the droplet on rough surfaces [12], and also a driving force for determining whether the droplet enters and wets the hole or not [13]. The contact area of the droplet is critical to its adhesion and spreading [14,15]. The inner pressure and surface tension can deform the solid materials, especially the soft materials, in the contact area and affects the dynamic wetting, spreading and transferring of the droplet [16–18].

The equilibrium shape of the droplet could be considered as part of a spherical surface [12,15,19–21] when the drop size is much smaller than the well-known capillary length [5] which can be given by $l_c = \sqrt{\gamma / \rho g}$, where, γ is liquid-air interface energy, ρ is the density of liquid, g is the gravitational acceleration. The effect of gravity should be taken into account when the drop size is larger than capillary length l_c (heavy droplets) [22–28]. The shape of droplet is determined by Laplace's equation, $2\gamma H = p_0 + \rho g z$, where H is the mean curvature, p_0 the pressure of apex of the droplet, z the vertical position below the apex. The exact shape of the droplet can be solved by using boundary conditions of a given volume of droplet and the contact angle θ. The exact shape is not readily determined because there is no analytical solution of the nonlinear differential governing equation. The equilibrium shape of heavy droplet is no longer a part of spherical surface on a flat or curved solid surface, but tends to become an oblate spheroid. The numerical results reveal that the equilibrium shape of a droplet is almost the shape of an axisymmetric ellipsoidal cap with

*Corresponding author (email: yuyang08@bit.edu.cn)

Young's contact angle below 120° [28].

Several models for the approximate solution were established recently. Erbil and Meric [23] studied the sessile drops on polymer surface by ellipsoid cap. Whyman and Bormashenko [25] established oblate spheroid droplet model to study the shape of heavy droplets. Other researchers analyzed the shape of droplet using an ellipsoidal cap shape which was obtained by free-energy minimization [28]. These models were established on a flat surface. However, the wetting behaviors of droplets on curved surfaces have also been investigated in recent decades, such as electrowetting on spherical surface [29], adjustable lenses [30], flexible paper-like substrates [31] and soft deformed membrane [17]. Therefore, we established axisymmetric ellipsoidal surface model with Young's contact angle to further investigate the equilibrium shape of heavy droplets on flat solid surfaces and spherical surfaces.

The static and quasi-static wetting phenomena can be well simulated by Surface Evolver (SE) [32]. Chou et al. [27] simulated the stable states of pendant droplets on fibers with gravitational effects and Chatain et al. [33] analyzed the shapes and energies of droplets on micro-patterned substrates. Others studied the shape of contact line on the surfaces with micro-posts and the stability of a bubble on superhydrophobic surfaces [34,35]. These studies reveal that the equilibrium shape of droplet can be obtained by SE simulation. We simulated the shape of droplet on flat, convex and concave curved surfaces by SE in order to check the precision and available range of our theoretical model.

2 Theoretical and numerical methods

2.1 Theoretical method

The coordinate origin is taken at the centre of ellipse, the x axis is along horizontal principle axis (a) of ellipse and the y axis along vertical principle axis (b). The point on ellipse can be represented as ($a\cos\phi$, $b\sin\phi$), and the angle between the solid surface and the tangent of elliptical arc at the solid surface is Young's contact angle (θ) as shown in Figure 1(a). The theoretical equilibrium shape of droplet can be predicted as the surface which is rotated by solid black curve along y axis. The solid black curve corresponds to the range of parameter $\phi \in (\phi_0, \pi/2)$, ϕ_0 is the starting angle and depends on contact angle θ and principle axes. According to this coordinate system, the mean curvature of ellipsoidal surface is $2b/a^2$ and $1/a + a/b^2$ at $y=b$ and $y=0$, respectively. The balance equation of pressure can be given as:

$$2\gamma\frac{b}{a^2}+\rho g b=\gamma\left(\frac{1}{a}+\frac{a}{b^2}\right). \tag{1}$$

The slope of elliptical arc at the solid surface is $k=\mathrm{d}y/\mathrm{d}x=-b/(a\tan\phi_0)=\tan(\pi-\theta)$. Thus the starting angle is

$$\phi_0=\arctan\left(\frac{b}{a\tan\theta}\right). \tag{2}$$

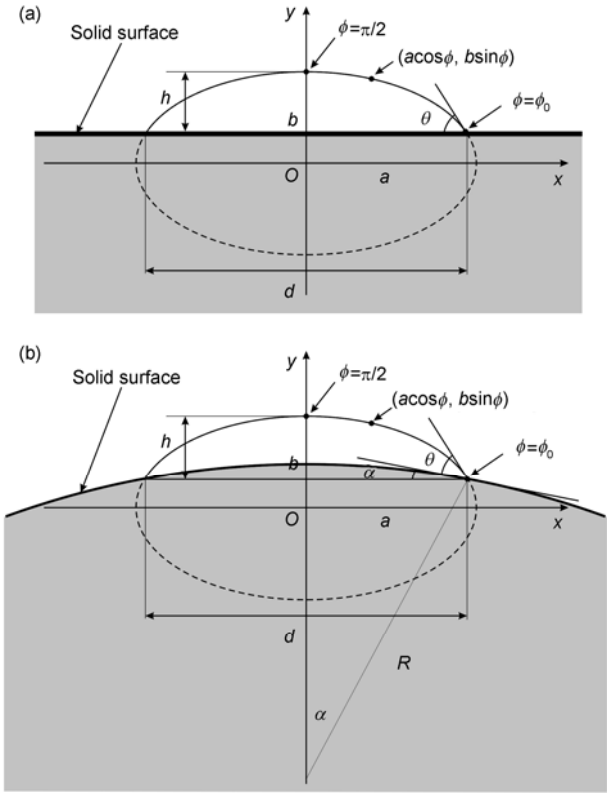

Figure 1 Ellipsoidal surface model with Young's contact angle and coordinate system. (a) Theoretical ellipsoidal model on flat surface; (b) theoretical ellipsoidal model on spherical surface.

The volume of heavy droplet can be expressed as:

$$V=\int_{\phi_0}^{\pi/2}\pi x^2\mathrm{d}y=\frac{1}{3}\pi a^2 b\left(\sin^3\phi_0-3\sin\phi_0+2\right). \tag{3}$$

We can solve for a, b and ϕ_0 from simultaneous eqs. (1)–(3) depending on the volume of liquid V, liquid-air interface energy γ, density of liquid ρ and wetting property (contact angle θ). Then the parameters, the height h of droplet and diameter of contact area d, can be obtained easily by: $h=b(1-\sin\phi_0)$, $d=2a\cos\phi_0$.

The contact angle also keeps constant when the droplet is on the convex spherical surface with radius R, as shown in Figure 1(b). The balance equation of pressure is the same as eq. (1). However, the slope of elliptical arc at the solid surface depends on the position and radius of the sphere as $k=\mathrm{d}y/\mathrm{d}x=-b/(a\tan\phi_0)=\tan[\pi-(\theta+\alpha)]$, where α is the central angle. The starting angle is

$$\phi_0=\arctan\left(\frac{b}{a\tan(\theta+\alpha)}\right). \tag{4}$$

The volume of heavy droplet on spherical surface can be expressed as:

$$V=\frac{1}{3}\pi a^2 b\left(\sin^3\phi_0-3\sin\phi_0+2\right)-\frac{1}{3}\pi R^3\left(\cos^3\alpha-3\cos\alpha+2\right). \quad (5)$$

And the geometric condition is

$$a\cos\phi_0=R\sin\alpha. \quad (6)$$

We can solve for a, b and ϕ_0 from simultaneous eqs. (1) and (4)–(6) in order to be used to predict the equilibrium shape of droplet on convex spherical surface. If the droplet is on concave spherical surface with the radius R, the radius R will have a negative value for eqs. (5) and (6).

2.2 Simulation method

The basic idea of SE is to minimize the free energy of system subject to the constraints. The stable shape of droplet with minimum free energy corresponds to the equilibrium shape. The total free energy of sessile droplet on surface includes solid-liquid (γ_{SL}), solid-air (γ_{SA}) and liquid-air (γ) interface energy and gravitational energy. Simplifying the total free energy by the well-known Young's equation $\cos\theta=(\gamma_{SA}-\gamma_{SL})/\gamma$, it can be given as:

$$E=\sum_i(\gamma A_{LA}^i)+\sum_j(-\gamma A_{SL}^j\cos\theta)+\sum_k(\rho g V^k z^k), \quad (7)$$

where A_{LA}^i and A_{SL}^j are liquid-air and solid-liquid interfacial areas, respectively. The V^k and z^k are the volume and the centroid position of each liquid element, respectively.

The initial model was established with calculating parameters density of liquid 1000 kg/m^3, gravitational acceleration 9.8 m/s^2, liquid-air interface energy 0.07275 J/m^2, and the volume of liquid 60 μL and contact angle of surface 57° for Figure 2(a), the volume of liquid 100 μL and contact angle of surface 106° for Figure 2(b), respectively. Two

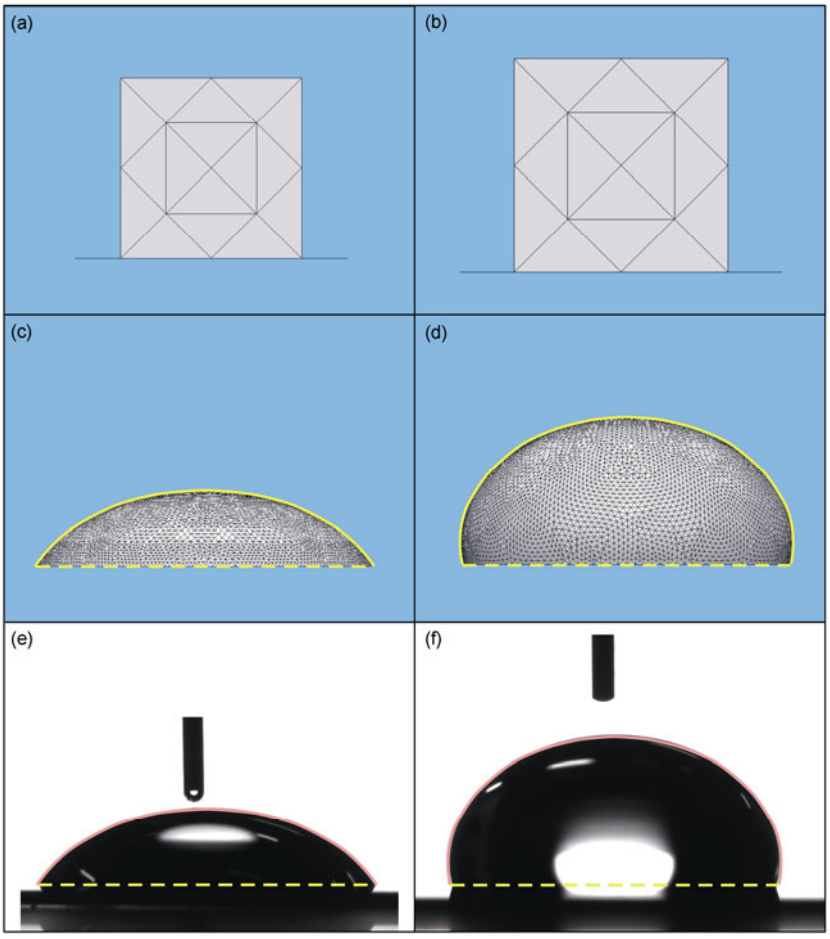

Figure 2 (Color online) Simulation results by SE in comparison with experimental results. (a) Initial model of a 60 μL droplet on the surface with contact angle 57°; (b) initial model of a 100 μL droplet and contact angle 106°; (c) and (d) simulation results corresponding to (a) and (b), respectively; (e) experimental observation of a 60 μL droplet on the surface with contact angle 57° by OCA 20 Device from Dataphysics (Germany); (f) experimental observation of a 100 μL droplet and contact angle 106°.

constraints were used, the vertices and edges of the contact area were required to lie on the flat or spherical surface and the droplet volume was kept constant during iteration. The simulations were performed by SE to evolve the configuration of liquid from the initial model to that with minimum system energy. Our calculation was performed until the total free energy difference converges to within the acceptable tolerance of 10^{-4} when we considered it is at minimum system energy. The results were shown in Figures 2(c) and (d) corresponding to the initial model as Figures 2(a) and (b), respectively.

The shape of the droplet can be described through the coordinate of nodes on the liquid-air interface. The height and diameter of contact area of equilibrium droplet can also be obtained through these node data.

3 Results and discussion

We did simple wetting experiments at 20°C temperature and 55% humidity that a 60 μL water droplet is stably on flat silicon wafer with a contact angle 57° (Figure 2(e)). A 100 μL water droplet is stable on the flat silicon wafer coating Octadecyltricholorosilane (OTS) with the contact angle 106° (Figure 2(f)). The solid lines are the simulation shape (Figures 2(c) and (d)) by SE with the same volume and contact angle. It shows that the solid line edges fit the equilibrium shape of water droplet consistently. This allowed us to confirm the correctness of the SE simulation, so that we can check the available range of our theoretical model through the simulation results.

The shape of droplet with different liquid volumes and contact angles on flat surface had been theoretically obtained as shown in Figure 3. The solid line is theoretical ellipsoidal surface. It reveals that the theoretical model can predict when the liquid with small volume is stable on the hydrophilic surface (Figures 3(a)–(d)). The errors increases on hydrophobic surfaces (Figure 3(e)) and theoretical result is inconsistent on superhydrophobic surfaces (Figure 3(f)). It is much complicated to compare every point on the equi-

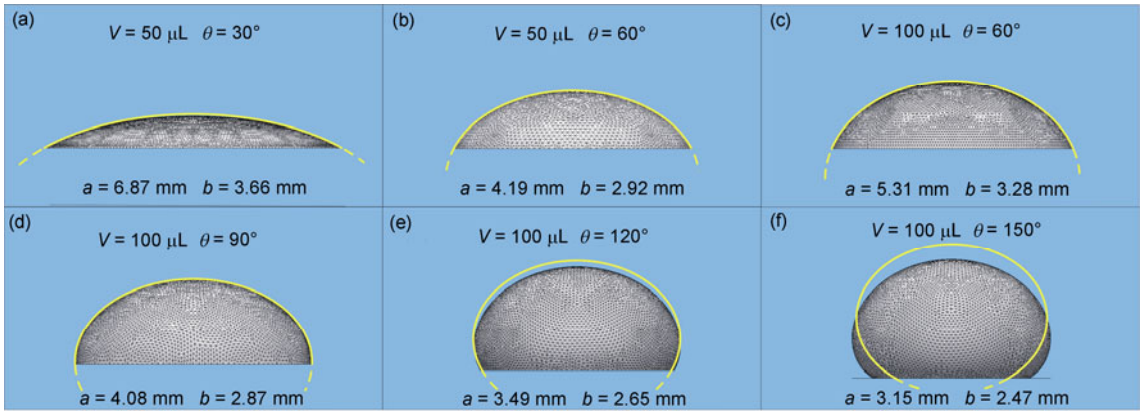

Figure 3 (Color online) Equilibrium shapes of heavy droplets and fitting elliptical surfaces (solid curves). a and b are the length of principle axes of fitting elliptical surfaces, respectively. (a) A 50 μL droplet on the surface with contact angle 30°; (b) a 50 μL droplet and contact angle 60°; (c) a 100 μL droplet and contact angle 60°; (d) a 100 μL droplet and contact angle 90°; (e) a 100 μL droplet and contact angle 120°; (f) a 100 μL droplet and contact angle 150°.

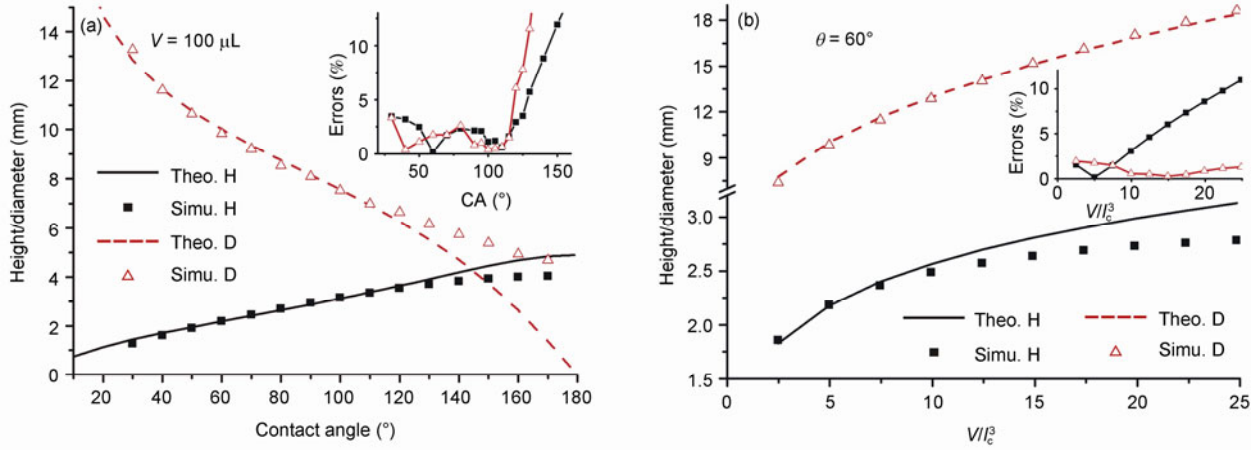

Figure 4 (Color online) Theoretical predictions of the height and diameter of contact area in comparison with the simulation results. (a) Theoretical and simulation results of the height and diameter vs. contact angle with constant 100 μL volume (errors changes as per the illustration); (b) theoretical and simulation results of the height and diameter vs. dimensionless volume with constant contact angle 60° (errors changes as per the illustration).

librium shape with the theoretical results. We found that the theoretical ellipsoidal surface could fit the equilibrium shape of droplet by SE simulation when the height and diameter of contact area both are consistent to the simulation, respectively. These two parameters are selected to analyze the errors in this paper. The theoretical and simulative height and diameter are shown in Figures 4(a) and (b) with different contact angles and volumes, respectively. The results show that the available range of our model (errors < 5%) for the contact angle is below 120° and the dimen-

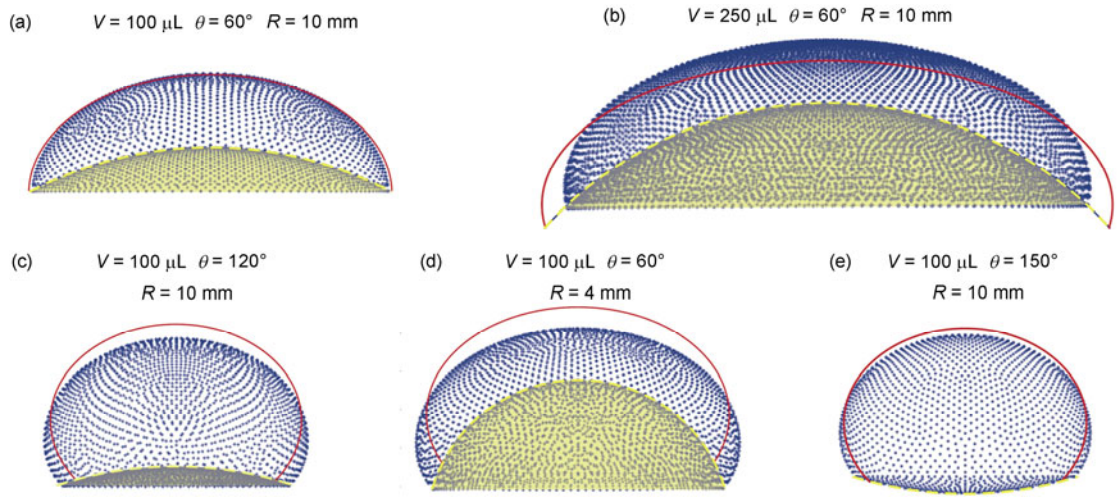

Figure 5 Simulative equilibrium shapes of heavy droplets on convex and concave surface by SE. The solid red lines are theoretical results. (a) Fitting is consistent in the available range; (b)–(d) fitting is not consistent with high volume liquid, large contact angle and high curvature, respectively, on convex surface; (e) fitting is not consistent until the contact angle is 150° on concave surface.

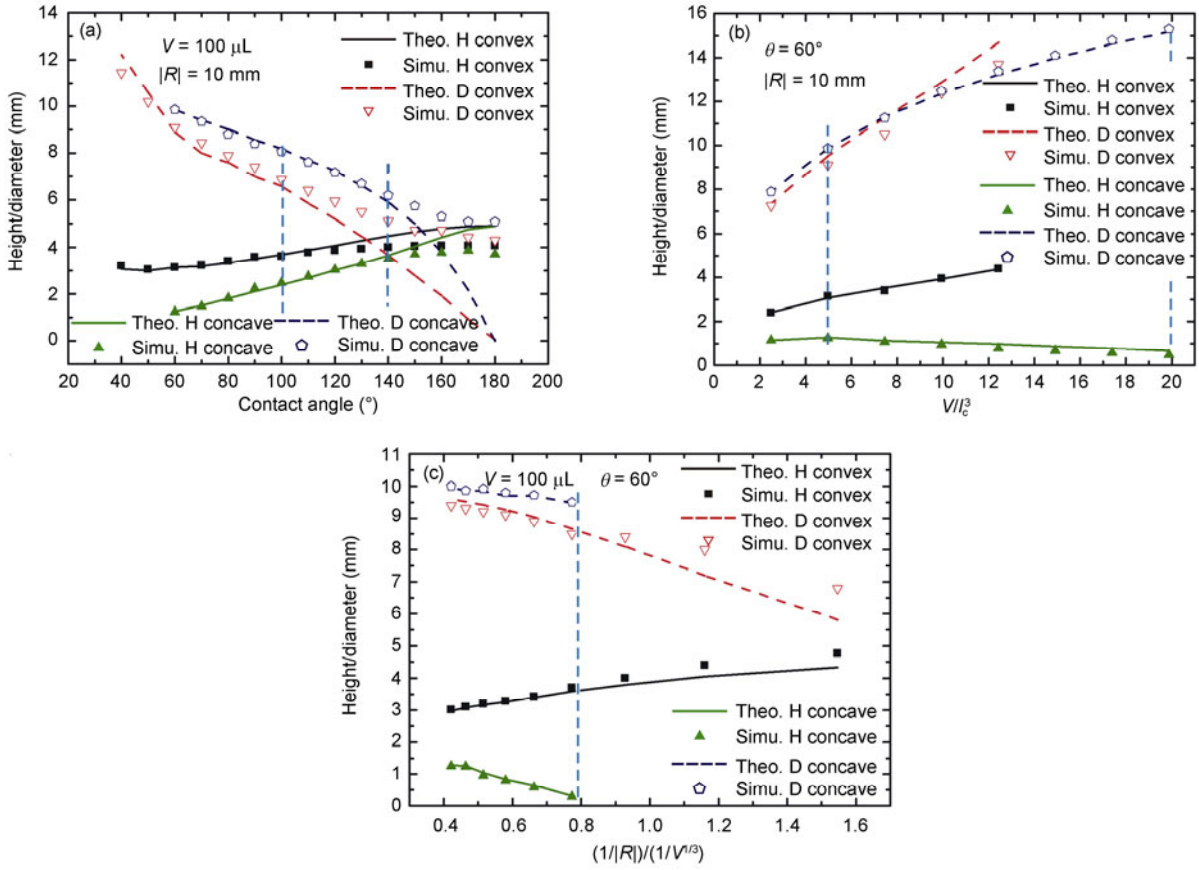

Figure 6 Theoretical and simulative results of the height and diameter on convex and concave surface. (a) Changes with contact angle; (b) changes with dimensionless volume; (c) changes with dimensionless curvature.

sionless volume of droplet (V/l_c^3) is less than 12, as the illustration in Figures 4(a) and (b) shows. This available range of our model is very similar to the results of Lubarda and Talke [28] in that the contact angle is below 120° and the droplet size is on the order of capillary length. Our model has the characteristic that the contact angle is constant (keeping the inherence wetting property of materials), the calculations are simple and the precision is good in available range. Our predictions are not as consistent as that of Lubarda and Talke [28] when the parameters are beyond available range. The model suggested by Lubarda and Talke [28] is based on the principle of free energy minimization, but the contact angle can not be kept constant on the solid surface. The calculation of free energy minimization was more complex than that of our model.

The equilibrium shape of droplet on spherical surfaces were theoretically obtained and compared with simulation results as illustrated in Figure 5. Only the nodes of surface of equilibrium shape are shown so that the solid spherical surface can be seen (the edges of spherical surface were marked by dash line). It reveals that the theoretical result is in good agreement when the parameters used in the available range (Figure 5(a)), but is inconsistent with a high volume of liquid (Figure 5(b)), large contact angle (Figure 5(c)) and small radius of convex spherical surface (high curvature, Figure 5(d)). It is more consistent for the droplet on concave spherical surface than on flat or convex spherical surface with the same volume and contact angle (Figure 5(e)).

The two parameters (height and diameter of contact area) are also used to check the available range of convex spherical model and concave spherical model as illustrated in Figure 6. The available contact angle ranges of the convex (R=10 mm) and concave (R=–10 mm) surface model are below 100° and 140° (Figure 6(a)), respectively using a 100 μL droplet. The available dimensionless volume ranges of convex (R=10 mm) and concave (R=–10 mm) surface model are less than 5 and 20 (Figure 6(b)), respectively, with the contact angle at 60°. It indicates that the available range changes are smaller for convex surface model and larger for concave surface model, in contrast to that of the flat surface model. The curvature of spherical surface certainly has an effect on available range. The available range of contact angle will be below 60° with 100 μL droplet when the dimensionless curvature $(1/R)/(1/V^{1/3})$ is more than 0.8. That is, the radius of convex spherical surface is less than 6 mm (Figure 6(c)). The droplet will be trapped in the concave spherical surface with the radius near to the characteristic length of droplet ($\sim V^{1/3}$), so that the theoretical prediction and simulation is terminated.

Currently, the theoretical ellipsoid model can not properly predict the shape of heavy droplet on hydrophobic surface on flat surface and spherical surface because the theoretical model has upper-lower symmetric, but the true shape of the heavy droplet does not. This new theoretical asymmetric model will be carried out for improving the model on hydrophobic surface in the future work.

4 Conclusion

Theoretical model of equilibrium shape of heavy droplet on flat and spherical solid surfaces were established and the equilibrium shape of droplet was simulated by SE. The contrasting results show that the flat surface model with Young's contact angle fit the equilibrium shape of heavy droplet consistently. The available range of our theoretical model was quantitatively analyzed by the characteristic parameters including height of droplet and diameter of contact area. The available range of this simply model does not decrease in contrast to the model of Lubarda and Talke. The model has the characteristic that the contact angle is constant, calculations are simple and the precision is in good agreement within the available range.

The theoretical model on spherical surface also fits the equilibrium shape of heavy droplets within the available range. It shows that the available range will decrease and increase on convex and concave spherical surface, respectively, in contrast to that of flat surface. The more the available range decreases, the higher curvature the convex spherical surface becomes.

This work was supported by the National Natural Science Foundation of China (Grant No. 10902015) and the Research Funds for the Doctoral Program of Higher Education of China (Grant No. 20091101120001). We acknowledge the helpful discussions with Prof. JI BaoHua at the Beijing Institute of Technology.

1 del Rio O I, Neumann A W. Axisymmetric drop shape analysis: Computational methods for the measurement of interfacial properties from the shape and dimensions of pendant and sessile drops. J Colloid Interface Sci, 1997, 196(2): 136–147
2 Perez M, Brechet Y, Salvo L, et al. Oscillation of liquid drops under gravity: Influence of shape on the resonance frequency. Europhys Lett, 1999, 47(2): 189–195
3 Sakai H, Fujii T. The dependence of the apparent con-tact angles on gravity. J Colloid Interface Sci, 1999, 210(1): 152–156
4 Chatterjee J. Limiting conditions for applying the spherical section assumption in contact angle estimation. J Colloid Interface Sci, 2003, 259(1): 139–147
5 de Gennes P G, Brochard-Wyart F, Quere D. Capillarity and Wetting Phenomena. Berlin: Springer, 2003
6 Aussillous P, Quere D. Properties of liquid marbles. Proc R Soc A-Math Phys Eng Sci, 2006, 462(2067): 973–999
7 Tadmor R, Yadav P S. As-placed contact angles for sessile drops. J Colloid Interface Sci, 2008, 317(1): 241–246
8 Wang F C, Feng J T, Zhao Y P. The head-on colliding process of binary liquid droplets at low velocity: High-speed photography experiments and modeling. J Col-loid Interface Sci, 2008, 326(1): 196–200
9 Tadmor R, Bahadur P, Leh A, et al. Measurement of lateral adhesion forces at the interface between a liquid drop and a substrate. Phys Rev Lett, 2009, 103(26): 266101
10 Su Y, Ji B, Huang Y, et al. Nature's design of hierarchical superhydrophobic surfaces of a water strider for low adhesion and low-en-

ergy dissipation. Langmuir, 2010, 26(24): 18926–18937
11 Su Y, Ji B, Zhang K, et al. Nano to micro structural hierarchy is crucial for stable superhydrophobic and water-repellent surfaces. Langmuir, 2010, 26(7): 4984–4989
12 Zheng Q S, Yu Y, Zhao Z H. Effects of hydraulic pressure on the stability and transition of wetting modes of superhydrophobic surfaces. Langmuir, 2005, 21(26): 12207–12212
13 Ng T W, Yu Y, Tan H Y, et al. Capillary well microplate. Appl Phys Lett, 2008, 93(17): 174105
14 Marmur A. The lotus effect: Superhydrophobicity and metastability. Langmuir, 2004, 20(9): 3517–3519
15 Yu Y, Zhao Z H, Zheng Q S. Mechanical and superhydrophobic stabilities of two-scale surfacial structure of lotus leaves. Langmuir, 2007, 23(15): 8212–8216
16 Shanahan M E R, Carre A. Spreading and dynamics of liquid drops involving nanometric deformations on soft substrates. Colloids Surf A-Physicochem Eng Asp, 2002, 206(1-3): 115–123
17 Yu Y S, Zhao Y P. Elastic deformation of soft membrane with finite thickness induced by a sessile liquid droplet. J Colloid Interface Sci, 2009, 339(2): 489–494
18 Tadmor R. Approaches in wetting phenomena. Soft Matter, 2011, 7(5): 1577–1580
19 Barthlott W, Neinhuis C. Purity of the sacred lotus, or escape from contamination in biological surfaces. Planta, 1997, 202(1): 1–8
20 Patankar N A. On the modeling of hydrophobic contact angles on rough surfaces. Langmuir, 2003, 19(4): 1249–1253
21 Patankar N A. Transition between superhydrophobic states on rough surfaces. Langmuir, 2004, 20(17): 7097–7102
22 Blokhuis E M, Shilkrot Y, Widom B. Youngs law with gravity. Mol Phys, 1995, 86(4): 891–899
23 Erbil H Y, Meric R A. Evaporation of sessile drops on polymer surfaces: Ellipsoidal cap geometry. J Phys Chem B, 1997, 101(35): 6867–6873
24 Larher Y. A very simple derivation of Young's law with gravity using a cylindrical meniscus. Langmuir, 1997, 13(26): 7299–7300
25 Whyman G, Bormashenko E. Oblate spheroid model for calculation of the shape and contact angles of heavy droplets. J Colloid Interface Sci, 2009, 331(1): 174–177
26 Ren H W, Xu S, Wu S T. Effects of gravity on the shape of liquid droplets. Opt Commun, 2010, 283(17): 3255–3258
27 Chou T H, Hong S J, Liang Y E, et al. Equilibrium phase diagram of drop-on-fiber: Coexistent states and gravity effect. Langmuir, 2011, 27(7): 3685–3692
28 Lubarda V A, Talke K A. Analysis of the equilib-rium droplet shape based on an ellipsoidal droplet model. Langmuir, 2011, 27(17): 10705–10713
29 Wang Y, Zhao Y P. Electrowetting on curved surfaces. Soft Matter, 2012, 8(9): 2599–2606
30 Kuiper S, Hendriks B H W. Variable-focus liquid lens for miniature cameras. Appl Phys Lett, 2004, 85(7): 1128–1130
31 Rogers J A, Bao Z, Baldwin K, et al. Paper-like electronic displays: Large-area rubber-stamped plastic sheets of electronics and microencapsulated electrophoretic inks. Proc Nat Acad Sci USA, 2001, 98(9): 4835–4840
32 Brakke K A. The surface evolver. Exp Math, 1992, 1(2): 141–165
33 Chatain D, Lewis D, Baland J P, et al. Numerical analysis of the shapes and energies of droplets on micropatterned substrates. Langmuir, 2006, 22(9): 4237–4243
34 Dorrer C, Ruehe J. Contact line shape on ultra-hydrophobic post surfaces. Langmuir, 2007, 23(6): 3179–3183
35 Ling W Y L, Lu G, Ng T W. Increased stability and size of a bubble on a superhydrophobic surface. Langmuir, 2011, 27(7): 3233–3237